 doi:10.20944/preprints202103.0326.v2

Displacement Formulations for Deformation and Vibration of Elastic Circular Torus

Bohua Sun[1]

[1]*Institute of Mechanics and Technology & School of Civil Engineering, Xi'an University of Architecture and Technology, Xi'an 710055, China*
http://imt.xauat.edu.cn
email: sunbohua@xauat.edu.cn

The formulation used by most of the studies on an elastic torus are either Reissner mixed formulation or Novozhilov's complex-form one, however, for vibration and some displacement boundary related problem of a torus, those formulations face a great challenge. It is highly demanded to have a displacement-type formulation for the torus. In this paper, I will carry on my previous work [B.H. Sun, Closed-form solution of axisymmetric slender elastic toroidal shells. J. of Engineering Mechanics, 136 (2010) 1281-1288.], and with the help of my own maple code, I am able to simulate some typical problems and free vibration of the torus. The numerical results are verified by both finite element analysis and H. Reissner's formulation. My investigations show that both deformation and stress response of an elastic torus are sensitive to the radius ratio, and suggest that the analysis of a torus should be done by using the bending theory of a shell, and also reveal that the inner torus is stronger than outer torus due to the property of their Gaussian curvature. Regarding the free vibration of a torus, our analysis indicates that both initial in u and w direction must be included otherwise will cause big errors in eigenfrequency. One of the most intestine discovery is that the crowns of a torus are the turning point of the Gaussian curvature at the crown where the mechanics' response of inner and outer torus is almost separated.

Keywords: circular torus, deformation, vibration, Gauss curvature, Maple

I. INTRODUCTION

Many natural and man-made objects take the shape of torus, doughnut and tube (shown in Fig. 1) might be two of most popular torus.

FIG. 1: Doughnut and tube.

The torus or toroidal shell, in full or partial geometric form, is widely used in structural engineering (Chang(Zhang) 1949 [1], Qian and Liang 1979 [2], Xia and Zhang 1986 [3], Zhang, Ren and Sun 1990 [4], Zhang and Zhang 1991 [5], 1994 [6], Audoly and Pomeau 2010 [7], Sun 2010 [8] 2012 [9], Clark 1950 [10, 11], Dahl 1953 [12], Novozhilov 1959 [13], Timoshenko and Woinowsky-Krieger 1959 [14], Flügge 1973 [15], Gol'denveizer 1961 [16] Sun 2013 [17], Föppl 1907 [18] Weihs 1911 [19], Wissler 1916 [20], Kuznetsov and Levyakov 2001 [21], Zingoni, Enoma and Govender 2015 [22], Jiammeepreecha and Chucheepsakul 2017 [23], Enoma and Zingoni 2020 [24], H. Reissner 1912 [25], Meissner 1915 [26], Tölke 1938 [27], E. Reissner 1949 [28], Tao 1959 [29], Steele 1965 [30], Sun 2018 [31], Sun 2020 [32]).

Among regular shells, such as circular cylindrical shells, conical shells, spherical shells, and tori, the deformation of the torus is one of the most difficulty topics due to its complicated topology, where the torus geometry has both Positive, negative Gaussian curvature and turning points.

The torus has been studied for more than 110 years ((Chang(Zhang) 1949 [1], Qian and Liang 1979 [2], Xia and Zhang 1986 [3], Zhang, Ren and Sun 1990 [4], Zhang and Zhang 1991 [5], 1994 [6], Audoly and Pomeau 2010 [7], Sun 2010 [8] 2012 [9], Clark 1950 [10, 11], Dahl 1953 [12], Novozhilov 1959 [13], Föppl 1907 [18] Weihs 1911 [19], Wissler 1916 [20], H. Reissner 1912 [25], Meissner 1915 [26], Tölke 1938 [27], E. Reissner 1949 [28], Tao 1959 [29], Steele 1965 [30], Sun 2018 [31], Sun 2020 [32], Sun 2021 [33], Sun [34]), and various aspects have been extensively investigated. In this paper, we will restrict ourselves to the small symmetrical deformation of elasic torus with a circular cross-section, and in particular with an emphasis on its theoretical formulation, associated analytical and numerical solutions. We will not touch topics such as non-circular cross-section, buckling, vibration, membrane solutions, and finite element analysis, which can be seen in the literature [21–24].

When the torus was first studied, high-order and complicated governing equations of a torus under symmetric

Preprints (www.preprints.org) | NOT PEER-REVIEWED | Posted: 25 January 2022 doi:10.20944/preprints202103.0326.v2

loads were reduced to lower-order, ordinary differential equation (ODE) by Hans Reissner (1912)[25] when he was a professor at ETH in Switzerland. His colleague at ETH, Meissner (1915) [26] derived a complex-form equations for the shell of revolution. Hence, the first complex-form equation of the shells of revolution including torus is called the Reissner-Meissner equation, which is a ODE system about shear force Q and rotation χ (Flügge 1973 [15]). In 1959, Novozhilov published his celebrated monograph on the complex-form theory of shells, and formulated symmetrical deformation of a torus in his complex-form (Novozhilov 1959 [13]).

Regarding formulation of elastic torus, governing equations that all publications adopted are either Reissner-Meissner's mixed formulation or Novozhilov's complex-form one. Although those formulations have some advantages, however they can not be used for vibration analysis and/or have difficulty when you have to deal with displacement boundary conditions. Therefore, it is desired to have displacement formulations for elastic torus. Sun 2010 [8] who derived displacement-type equations for torus and obtained a closed-form solution for special case as radius ratio $\frac{a}{R} \to 0$. This special solution can not capture full mechanics nature of torus and therefore are needed to be improved further.

This study wishes to carry on my previous works (Sun 2010 [8]), and investigates mechanical response for arbitrary ratio $\frac{a}{R}$. The content is organised as follows: Section 2 reformulate displacement-type formulation of torus. Section 3 applies the displacement formulation to three problems. The first and 3rd problem can be calculated by both Reissner's and Novozhilov's formulation, while the 2nd can not be solved by any exiting formulation of torus except displacement-type one. For numerical simulation, we write a general code by Maple. Section 4 obtains eigenfrequency and eigenmode. Section 5 verifies our results by both finite element analysis and Hans Reissner's formulation. Section 6 provides conclusions.

II. DISPLACEMENT-TYPE FORMULATION OF SYMMETRICAL DEFORMATION OF ELASTIC TORUS

The displacement-type formulation was derived by Sun 2010 [8, 9], but for completeness of representation, we will reformulate again in this section using different notations. For convenience of readers, all quantities notation and definition please refers to well-known book of J.N. Reddy 2007 [38].

For the torus shown in Fig. 3, the positions of points on the middle surface will be determined by the angles θ and φ. Further, let R_1 be the radius of curvature of the meridian and R_2 the radius of curvature of the normal section, tangential to the parallel circle. This second radius is equal to the segment of the perpendicular to the middle surface between this surface and the axis of the torus.

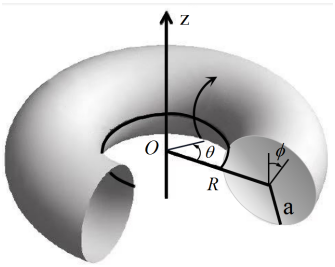

FIG. 2: Torus geometry and cross-sectional. Principal radii of curvature are $R_1 = a$ and $R_2 = a + \frac{R}{\sin\phi}$; principal curvature $K_1 = \frac{1}{a}$, $K_2 = \frac{\sin\phi}{R + a\sin\phi}$; Gauss curvature $K = K_1 K_2 = \frac{\sin\phi}{a(R + a\sin\phi)}$.

The Lamé parameters of torus shown in Fig.2 are determined by the expressions

$$a_1 = R_1 = a,\ a_2 = R_2 \sin\phi = R + a\sin\phi. \tag{1}$$

The principal radii of curvature are given by

$$R_1 = a,\ R_2 = \frac{R + a\sin\phi}{\sin\phi} \tag{2}$$

Regarding the forces shown in Fig.3, the balance equations are

$$\begin{aligned} \frac{d}{d\phi}(rN_{\phi\phi}) - N_{\theta\theta}R_1\cos\phi + rQ_\phi + R_1 r f_\phi = 0, \\ \frac{d}{d\phi}(rQ_\phi) - R_1 r(\frac{N_{\phi\phi}}{R_1} + \frac{N_{\theta\theta}}{R_2}) + R_1 r f_\zeta = 0, \end{aligned} \tag{3}$$

where $r = R_2\sin\phi = R + a\sin\phi$, distributed loads f_ϕ, f_ζ along ϕ, ζ direction, and shear force

$$Q_\phi = \frac{1}{R_1 r}\frac{d}{d\phi}(rM_{\phi\phi}) - \frac{1}{r}\cos\phi M_{\theta\theta}. \tag{4}$$

where the resultant membranae forces are $N_{\phi\phi} = K(\varepsilon_{\phi\phi} + \nu\varepsilon_{\theta\theta})$, $N_{\theta\theta} = K(\nu\varepsilon_{\phi\phi} + \varepsilon_{\theta\theta})$, and resultant bending moments are $M_{\phi\phi} = B(\kappa_{\phi\phi} + \nu\kappa_{\theta\theta})$, $M_{\theta\theta} = B(\nu\kappa_{\phi\phi} + \kappa_{\theta\theta})$; The membranae strains are $\varepsilon_{\phi\phi} = \frac{1}{R_1}(\frac{du}{d\phi} + w)$, $\varepsilon_{\theta\theta} = \frac{1}{R_2}(u\cot\phi + w)$, and change of curvature are $\kappa_{\phi\phi} = \frac{1}{R_1}\frac{d\varphi_\phi}{d\phi}$, $\kappa_{\theta\theta} = \frac{\cot\phi}{R_2}\varphi_\phi$, where total rotation $\varphi_\phi = \frac{1}{R_1}(u - \frac{dw}{d\phi})$; and membranae stiffness $K = \frac{Eh}{1-\nu^2}$, bending stiffness $B = \frac{Eh^3}{12(1-\nu^2)}$, thickness h, Young modulus E and Poisson's ratio ν.

With the above strains and curvature change, the resultant membranae force and bending moments can be

Preprints (www.preprints.org) | NOT PEER-REVIEWED | Posted: 25 January 2022 doi:10.20944/preprints202103.0326.v2

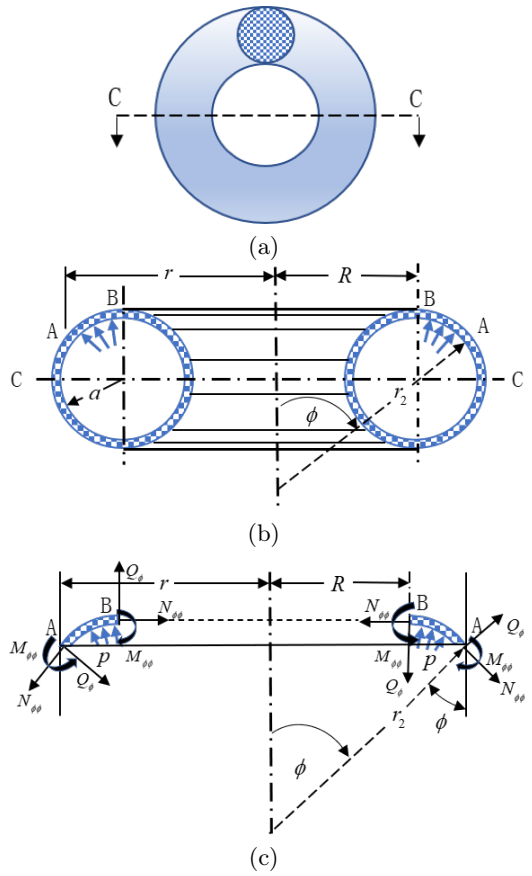

FIG. 3: Geometry of torus, loading, forces and moments

expressed in terms of displacements u, w as follows;

$$
\begin{aligned}
N_{\phi\phi} &= K[\frac{1}{R_1}(\frac{du}{d\phi}+w)+\nu\frac{1}{R_2}(u\cot\phi+w)],\\
N_{\theta\theta} &= K[\nu\frac{1}{R_2}(u\cot\phi+w)+\frac{1}{R_1}(\frac{du}{d\phi}+w)],\\
M_{\phi\phi} &= B[\frac{1}{R_1}\frac{d\varphi_\phi}{d\phi}+\nu\frac{\cot\phi}{R_2}\varphi_\phi]\\
&= B\left\{\frac{1}{R_1}\frac{d}{d\phi}(\frac{1}{R_1}(u-\frac{dw}{d\phi}))+\nu\frac{\cot\phi}{R_2}\frac{1}{R_1}(u-\frac{dw}{d\phi})\right\},\\
M_{\theta\theta} &= B[\nu\frac{1}{R_1}\frac{d\varphi_\phi}{d\phi}+\frac{\cot\phi}{R_2}\varphi_\phi]\\
&= B\left\{\nu\frac{1}{R_1}\frac{d}{d\phi}(\frac{1}{R_1}(u-\frac{dw}{d\phi}))+\frac{\cot\phi}{R_2}\frac{1}{R_1}(u-\frac{dw}{d\phi})\right\},
\end{aligned}
\tag{5}
$$

Substituting the shear force Q_ϕ in Eq.4 into Eq.3 and produce

$$
\begin{aligned}
&\frac{d}{d\phi}(rN_{\phi\phi})-N_{\theta\theta}R_1\cos\phi\\
&+\frac{1}{R_1}[\frac{d}{d\phi}(rM_{\phi\phi})-r\cos\phi M_{\theta\theta}]+R_1rf_\phi=0,\\
&\frac{d}{d\phi}[\frac{1}{r}\frac{d}{d\phi}(rM_{\phi\phi})-\cos\phi M_{\theta\theta}]\\
&-R_1r(\frac{N_{\phi\phi}}{R_1}+\frac{N_{\theta\theta}}{R_2})+R_1rf_\zeta=0,
\end{aligned}
\tag{6}
$$

The Eq. 6 can be further simplified by substituting the constitutive relations into Eq.bal-2, which will generate a final equations that is a six order ordinary differential equation system about displacement $u(\phi)$ and $w(\phi)$.

$$
\begin{aligned}
&K\frac{d}{d\phi}[(\frac{R}{a}+\sin\phi)(\frac{du}{d\phi}+w)+\nu\sin\phi(u\cot\phi+w)]\\
&-K\cos\phi[\nu\frac{a\sin\phi}{R+a\sin\phi}(u\cot\phi+w)+(\frac{du}{d\phi}+w)]\\
&+\frac{B}{a^2}\frac{d}{d\phi}[(\frac{R}{a}+\sin\phi)\frac{d}{d\phi}(u-\frac{dw}{d\phi})+\nu\cos\phi(u-\frac{dw}{d\phi})]\\
&-\frac{B}{a^2}\cos\phi[\nu(\frac{R}{a}+\sin\phi)\frac{d}{d\phi}(u-\frac{dw}{d\phi})+\cos\phi(u-\frac{dw}{d\phi})]\\
&+a(R+a\sin\phi)f_\phi=0,\\
&\frac{B}{a}\frac{d}{d\phi}\{\frac{1}{R+a\sin\phi}\frac{d}{d\phi}[(\frac{R}{a}+\sin\phi)\frac{d}{d\phi}(u-\frac{dw}{d\phi})\\
&+\nu\cos\phi(u-\frac{dw}{d\phi})]\\
&-\frac{B}{a}\frac{\cos\phi}{R+a\sin\phi}[\nu(\frac{R}{a}+\sin\phi)\frac{d}{d\phi}(u-\frac{dw}{d\phi})+\cos\phi(u-\frac{dw}{d\phi})]\}\\
&-K[\frac{R+a\sin\phi}{a}(\frac{du}{d\phi}+w)+\nu\sin\phi(u\cot\phi+w)]\\
&-Ka\sin\phi[\nu\frac{\sin\phi}{R+a\sin\phi}(u\cot\phi+w)+\frac{1}{a}(\frac{du}{d\phi}+w)]\\
&+a(R+a\sin\phi)f_\zeta=0.
\end{aligned}
\tag{7}
$$

Eq.7 is the final governing equations in terms of displacements u, w of elastic thin torus and was derived by Sun 2010 [8, 9].

III. NUMERICAL STUDIES OF SYMMETRICAL DEFORMATION OF TORUS

Eq. 7 will be solved numerically. Unless otherwise stated, numerical calculations in this paper are based on the data in Table I.

We vary the radius $a = 3k$, $k = 1, 2, 3$, while other quantities are unchanged. Table I lists the geometric and material properties of the torus.

Preprints (www.preprints.org) | NOT PEER-REVIEWED | Posted: 25 January 2022 doi:10.20944/preprints202103.0326.v2

TABLE I: Data of torus

Quantities	R	a	h	E	ν	M_0	Q_0
Units	m	m	m	N/m^2	1	Nm	N
Data	10	$3k$	$a/15$	2.07×10^{11}	0.3	1	1

Note: Loads are set to unit values in all simulations. Since a small deformation is a linear problem, the superposition principle can be used with different loads, and solutions obtained by multiplying our results by an appropriate factor.

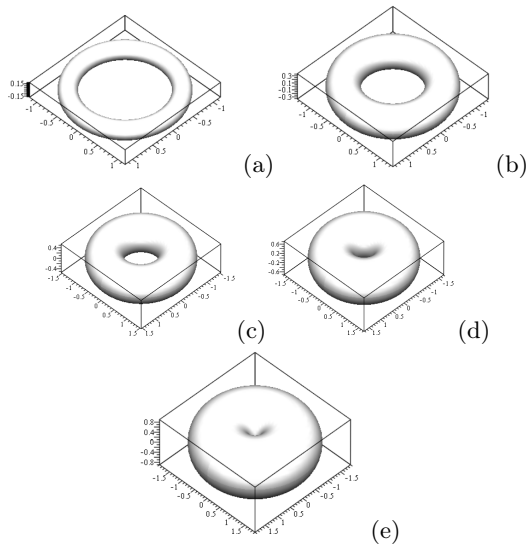

FIG. 4: Torus geometry with different radii $a = 0.18k[m]$ ($k = 1, 2, 3, 4, 5$)

For simplification of picture presentation of our results, physical units will not be plotted in all drawings. For this purpose, we list all physical units of in Table II:

TABLE II: Physical units

R	a	h	E	ν	$M_{\phi\phi}$, $M_{\theta\theta}$	$N_{\phi\phi}$, $N_{\theta\theta}$	Q_ϕ	$\sigma_{\phi\phi}$	u	w	Δ_z
m	m	m	N/m^2	1	Nm	N/m	N/m	N/m^2	m	m	m

Note: N is force physical unit and stands for Newton.

The geometry of these tori are shown in Fig. 4.

A. Complete torus with a penetrate cut along the parallel $\theta = \frac{\pi}{2}$ and loaded with vertical force Q_0

For a complete torus with a penetrate cut along the parallel $\theta = \frac{\pi}{2}$ and loaded with vertical force Q_0, the loading condition is shown in Fig. 5. The boundary condition is:

$$\theta = \frac{\pi}{2} : N_{\phi\phi} = -\frac{Q_0}{2\pi(R+a)},\ Q_\phi = 0,\ M_{\phi\phi} = 0, \quad (8)$$

$$\theta = -\frac{3\pi}{2} : N_{\phi\phi} = -\frac{Q_0}{2\pi(R+a)},\ Q_\phi = 0,\ M_{\phi\phi} = 0. \quad (9)$$

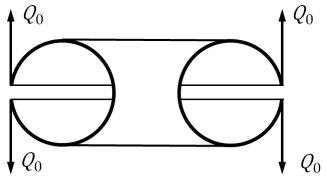

FIG. 5: Torus with a cut along its parallel at $\theta = \frac{\pi}{2}$ or $\theta = -\frac{\pi}{2}$ under load Q_0

A general code for this case is written by Maple [39]. With the help of the Maple code, some numerical results have been obtained and are shown in Fig. 6, 7, 8, and Fig. 9.

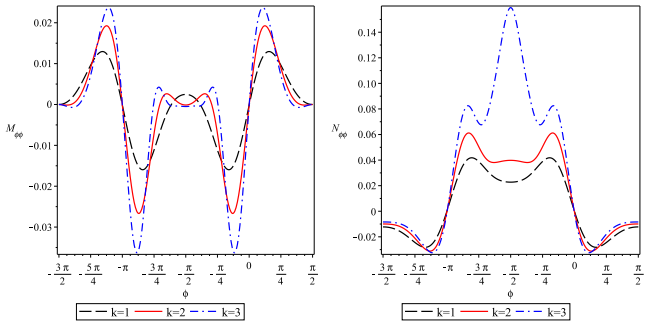

FIG. 6: Bending moments and membranes force for different radius $a = 3k[m]$. Left: Bending moment $M_{\phi\phi}$; Right: membranes force $N_{\phi\phi}$.

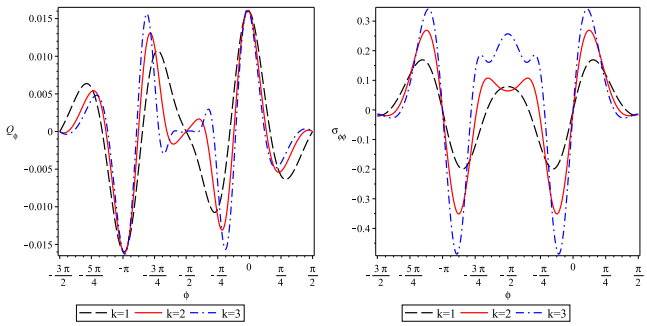

FIG. 7: Shear force for different radius $a = 3k[m]$. Left: Shear force Q_ϕ; Right: Stress σ_1.

The above all figures indicate that all quantities such as bending moments, surface forces, shear force, and displacement are strongly effected by the radius ratio $\alpha = a/R$, and vary dramatically with θ both near to and far from the edge. In particular, Fig. 9 reveals that the opening relative displacement Δ_z is mainly contributed by the deformation of outer torus ($\phi \in [0, \pi]$) while the most portion of inner torus ($\phi \in [0, -\pi]$) remains undeformed.

Preprints (www.preprints.org) | NOT PEER-REVIEWED | Posted: 25 January 2022 doi:10.20944/preprints202103.0326.v2

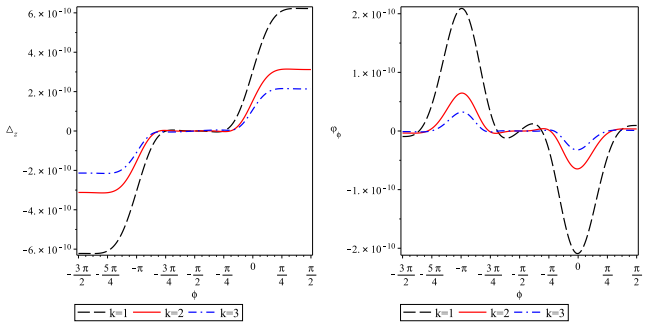

FIG. 8: Relative displacement in z direction Δ_z and rotation for different radius $a = 3k[m]$.

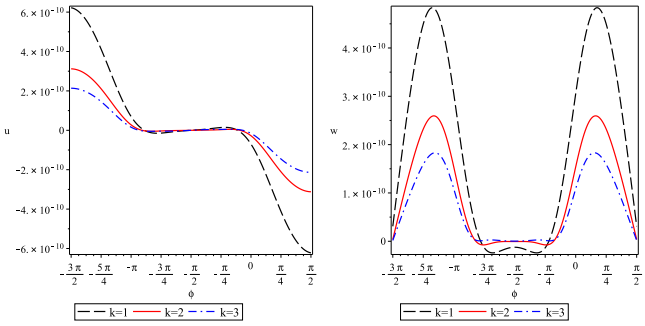

FIG. 9: u, w displacements in x, y direction for different radius $a = 3k[m]$.

B. Zhang's problem of torus (Chang 1944 [1])

In the Dr-Ing dissertation of W. Chang (later spell is changed to W. Zhang according to new Chinese spelling rule) (Chang 1944 [1]), he illustrated connection conditions for a problem as shown in Fig. 10:

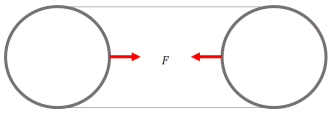

FIG. 10: Zhang's problem of torus: A self-balanced torus under a horizontal force in the inner portion.

However, Zhang did not give either analytical or numerical solutions of the problem. After revisiting Zhang's problem of torus, it is found that the reduced formulations such as Hans Reissner's mixed formulation and Novozhilov's complex-form ones are not able solve the problem, because both formulations can not provide a proper displacement and rotation boundary conditions. To the best of my knowledgeless, the study of this difficulty problem has not been seen in the literature and worth to be investigated.

If we cut the torus into two symmetrical parts as shown in Fig. 11.

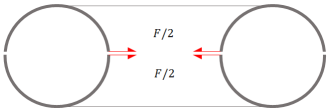

FIG. 11: Gutted torus in Zhang's problem.

Let's apply the displacement-form formulation to the bottom portion of the torus, ie., the portion within $\phi \in [\pi/2, 3\pi/2]$, and taking into account of symmetry, the shear force Q_1, displacement u and rotation $\frac{1}{a}(u - \frac{dw}{d\phi})$in two boundaries are:

$$\phi = \frac{\pi}{2} : u = 0, u - \frac{dw}{d\phi} = 0, Q_1 = 0, \tag{10}$$

$$\phi = \frac{3\pi}{2} : u = 0, u - \frac{dw}{d\phi} = 0, Q_1 = \frac{F}{4\pi R}. \tag{11}$$

The data of the torus is given in Table III:

TABLE III: Zhang's problem of torus (k=2,3) for

Quantities	R	a	h	E	ν	F
Units	m	m	m	N/m^2	1	N
Data	1	$0.2k$	$a/15$	2.07×10^{11}	0.3	1

We wrote a maple code for Zhang's problem of torus, and produced some results as shown in Fig. 12,13 and 14

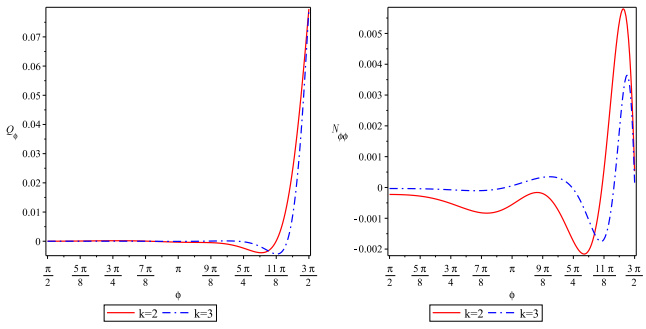

FIG. 12: Shear force and membrane force

The numerical studies show that the deformation is mainly contributed from the inner torus while outer torus almost undeformed. It seams that inner torus is separated from the outer one by the crowns (the turning point of the Gaussian curvature at $\phi = 0, \pi$).

To make sure the correctness of this discovery, let's investigate another version of Zhang's problem of torus as shown in Fig. 15:

The above numerical show that the turning point of the Gaussian curvature is the point of separation of me-

Preprints (www.preprints.org) | NOT PEER-REVIEWED | Posted: 25 January 2022 doi:10.20944/preprints202103.0326.v2

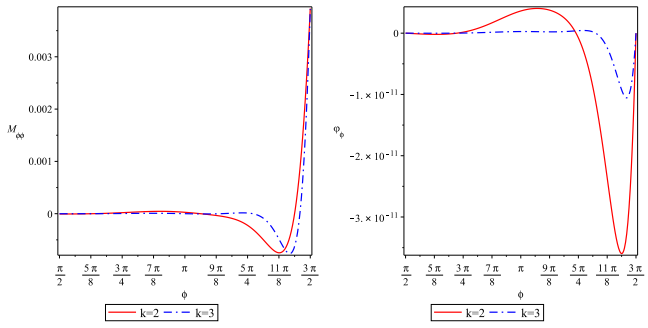

FIG. 13: Bending moments and rotation.

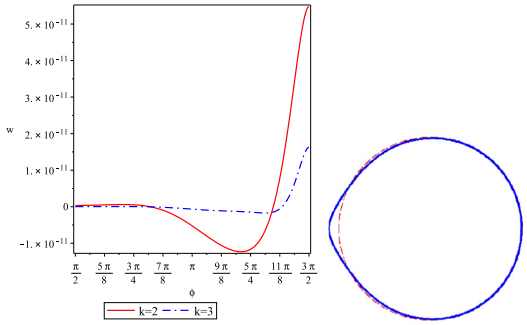

FIG. 14: Displacement w and deformed shape in blue.

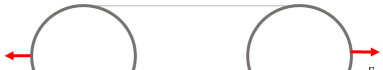

FIG. 15: Zhang's problem of torus.

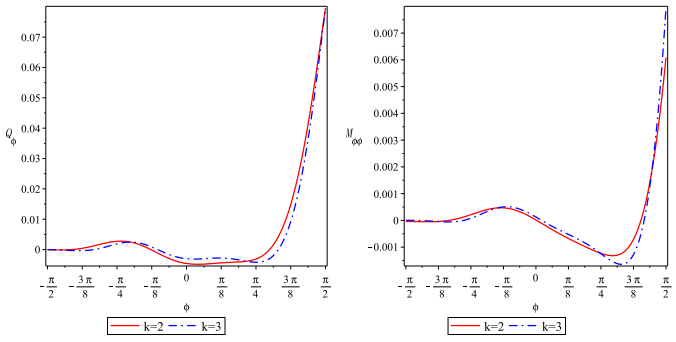

FIG. 16: Shear force and membrane force

chanics of torus, which can be used in architecture where you wish to change structural mechanics feature.

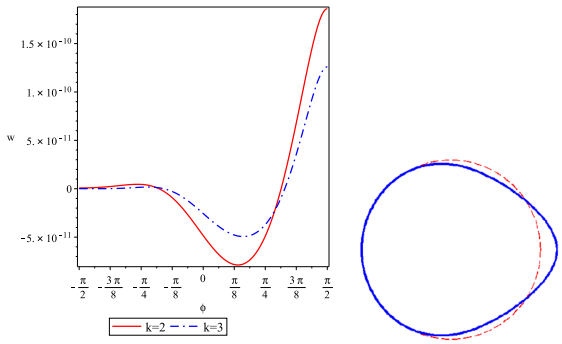

FIG. 17: Displacement w and deformed shape in blue.

C. Mechanical response difference between inner torus and outer torus loaded with vertical force

An inner torus loaded with vertical force as shown in Fig. 18:

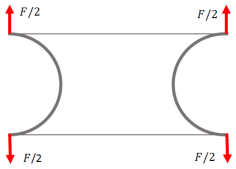

FIG. 18: A torus under a vertical force at the crowns.

Let's apply the displacement-form formulation to the inner torus, ie., the portion within $\phi \in [-\pi/2, 0]$, and taking into account of symmetry, the shear force Q_1, displacement u and rotation $\frac{1}{a}(u - \frac{dw}{d\phi})$ in two boundaries of the inner torus are :

$$\phi = 0 : \ M_{\phi\phi} = 0, \ N_{\phi\phi} = 0, \ Q_1 = \frac{F}{4\pi R}, \tag{12}$$

$$\phi = -\pi : \ M_{\phi\phi} = 0, \ N_{\phi\phi} = 0, \ Q_1 = -\frac{F}{4\pi R}, \tag{13}$$

The data of the torus is given in Table III. With the Maple code, we obtained some figures as shown in Fig. 19, 20, 21, 22 and 23.

An outer torus loaded with vertical force as shown in Fig. 24:

Let's apply the displacement-form formulation to the outer torus, ie., the portion within $\phi \in [0, \pi/2]$, and taking into account of symmetry, the shear force Q_1, displacement u and rotation $\frac{1}{a}(u - \frac{dw}{d\phi})$ in two boundaries of the inner torus are :

$$\phi = 0 : \ M_{\phi\phi} = 0, \ N_{\phi\phi} = 0, \ Q_1 = -\frac{F}{4\pi R}, \tag{14}$$

$$\phi = \pi : \ M_{\phi\phi} = 0, \ N_{\phi\phi} = 0, \ Q_1 = \frac{F}{4\pi R}, \tag{15}$$

Preprints (www.preprints.org) | NOT PEER-REVIEWED | Posted: 25 January 2022 doi:10.20944/preprints202103.0326.v2

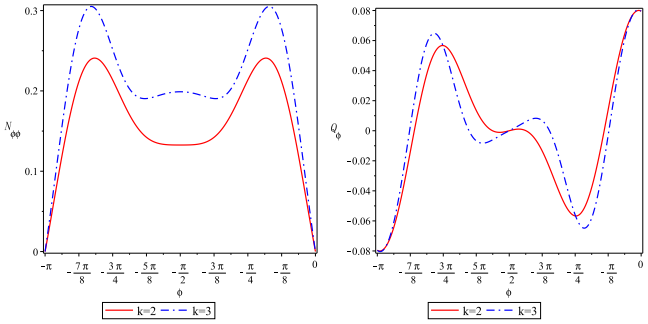

FIG. 19: Shear force and membrane force

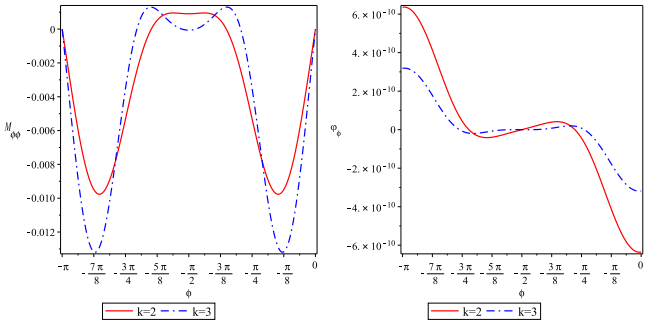

FIG. 20: Bending moments and rotation.

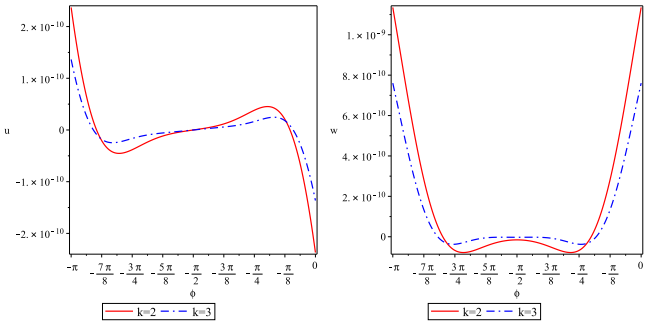

FIG. 21: Displacement u, w

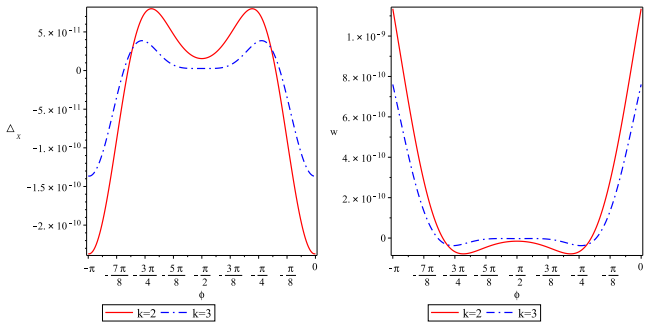

FIG. 22: Horizontal elongation and vertical shortening.

The data of the torus is given in Table III. With the Maple code, we obtained some figures as shown in Fig. 25, 26, 27, 28 and 29.

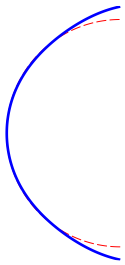

FIG. 23: Deformed shape of inner torus for $a = 0.4$.

If we compare the results of both inner and out torus, it is easy to discover that the inner torus is much stronger than the outer one under same loading condition. For

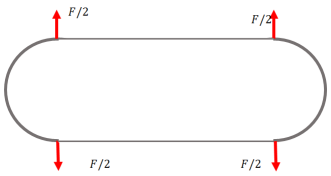

FIG. 24: A torus under a vertical force at the crowns.

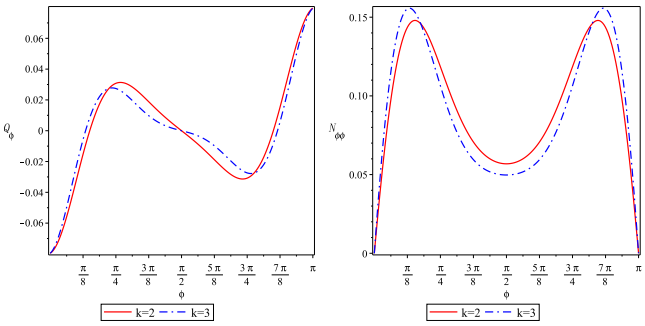

FIG. 25: Shear force and membrane force

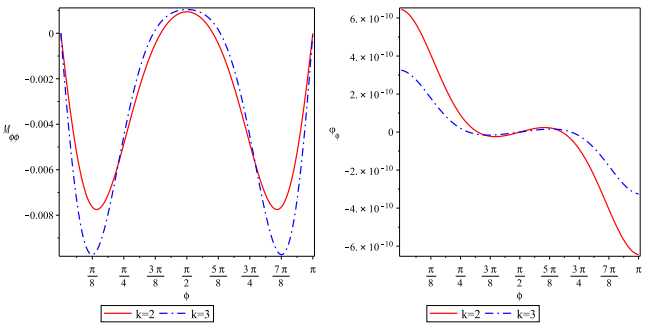

FIG. 26: Bending moments and rotation.

Preprints (www.preprints.org) | NOT PEER-REVIEWED | Posted: 25 January 2022 doi:10.20944/preprints202103.0326.v2

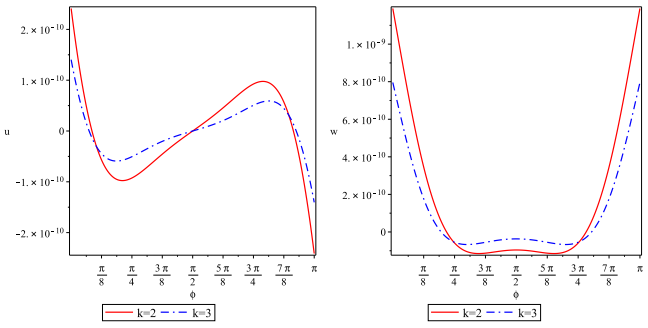

FIG. 27: Displacement u, w

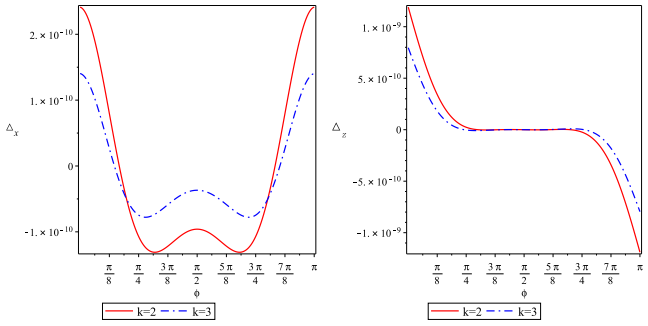

FIG. 28: Horizontal elongation and vertical shortening.

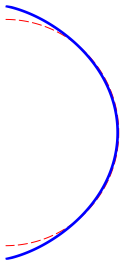

FIG. 29: Deformed shape of outer torus for $a = 0.4$.

instance, the vertical deformation or elongation:

$$Inner : \Delta_{inner} = 2.270682876 \times 10^{-9}[m] \quad (16)$$

$$Outer : \Delta_{outer} = 2.380005240 \times 10^{-9}[m]. \quad (17)$$

The deformation $\Delta_{inner} < \Delta_{outer}$ reveals that the inner torus is stronger or stiffer than the outer one under same loadings, the geometric reason behind this phenomena is that the Gaussian curvature of the inner torus is negative while the outer's Gaussian curvature is positive. Therefore, from structural mechanics point of view, the shape of inner torus should be the first option when you design a torus.

IV. FREE VIBRATION, EIGENFREQUENCY AND EIGENMODE OF ELASTIC TORUS

Besides finite element method, both Reissner's mixed formulation and complex-form one can not be used to deal with vibration of torus, because the acceleration of motion must be taken into account in the formulation. In this case, displacement-type formulation is the only one can be accepted. Therefore, in this section, we will study symmetric free vibration of the torus. In this case, the initial namely $-\rho h\frac{\partial^2 u}{\partial t^2}$ and $-\rho h\frac{\partial^2 w}{\partial t^2}$ must be introduced to the Eq. 7 and lead to a free vibration equation system of elastic torus as follows:

$$\begin{aligned}
&K\frac{\partial}{\partial\phi}[(\frac{R}{a}+\sin\phi)(\frac{\partial u}{\partial\phi}+w)+\nu\sin\phi(u\cot\phi+w)]\\
&-K\cos\phi[\nu\frac{a\sin\phi}{R+a\sin\phi}(u\cot\phi+w)+(\frac{\partial u}{\partial\phi}+w)]\\
&+\frac{B}{a^2}\frac{\partial}{\partial\phi}[(\frac{R}{a}+\sin\phi)\frac{\partial}{\partial\phi}(u-\frac{\partial w}{\partial\phi})+\nu\cos\phi(u-\frac{\partial w}{\partial\phi})]\\
&-\frac{B}{a^2}\cos\phi[\nu(\frac{R}{a}+\sin\phi)\frac{\partial}{\partial\phi}(u-\frac{\partial w}{\partial\phi})+\cos\phi(u-\frac{\partial w}{\partial\phi})]\\
&+a(R+a\sin\phi)(-\rho h\frac{\partial^2 u}{\partial t^2})=0,\\
&\frac{B}{a}\frac{\partial}{\partial\phi}\{\frac{1}{R+a\sin\phi}\frac{\partial}{\partial\phi}[(\frac{R}{a}+\sin\phi)\frac{\partial}{\partial\phi}(u-\frac{\partial w}{\partial\phi})\\
&+\nu\cos\phi(u-\frac{\partial w}{\partial\phi})]\\
&-\frac{B}{a}\frac{\cos\phi}{R+a\sin\phi}[\nu(\frac{R}{a}+\sin\phi)\frac{\partial}{\partial\phi}(u-\frac{\partial w}{\partial\phi})\\
&+\cos\phi(u-\frac{\partial w}{\partial\phi})]\}\\
&-K[\frac{R+a\sin\phi}{a}(\frac{\partial u}{\partial\phi}+w)+\nu\sin\phi(u\cot\phi+w)]\\
&-Ka\sin\phi[\nu\frac{\sin\phi}{R+a\sin\phi}(u\cot\phi+w)+\frac{1}{a}(\frac{\partial u}{\partial\phi}+w)]\\
&+a(R+a\sin\phi)(-\rho h\frac{\partial^2 w}{\partial t^2})=0,
\end{aligned} \quad (18)$$

where the mass density ρ and time t.

TABLE IV: Date of torus made of steel (k=1,2) for

Quantities	R	a	h	E	ν	ρ
Units	m	m	m	N/m^2	1	kg/m^3N
Data	1	$0.1k$	$a/15$	2.07×10^{11}	0.3	8050

For free vibration analysis, the displacement u, w be set as $[u, w] = [U(\phi), W(\phi)]\exp(i\omega t$, where ω is angular frequency, $U(\phi)$, $W(\phi)$ are the eigenmode of u, w, respectively. We have simulated the torus as shown in

Preprints (www.preprints.org) | NOT PEER-REVIEWED | Posted: 25 January 2022 doi:10.20944/preprints202103.0326.v2

Fig. 5 without load Q_0, which means that we are dealing with free vibration. With our general Maple code, eigenfrequencies are obtained as follows:

A. Taking into account of acceleration in both direction of u and w

For free vibration of torus, if we take into account of acceleration in both direction of u, w, namely $-\rho h\frac{\partial^2 u}{\partial t^2}$ and $-\rho h\frac{\partial^2 w}{\partial t^2}$. The eigenfrequences are obtained as follows:

$$a = 0.1[m] : \omega = 322.602[1/s] \quad (19)$$
$$a = 0.2[m] : \omega = 229.720[1/s]. \quad (20)$$

The eigenfrequency value indicates that the torus with smaller ratio a/R will generate higher frequency.

B. Taking into account of acceleration in direction of w

For free vibration of torus, if we only take into account of acceleration in direction of w, namely $-\rho h\frac{\partial^2 w}{\partial t^2}$. The eigenfrequency are obtained as follows:

$$a = 0.1[m] : \omega = 488.383[1/s] \quad (21)$$
$$a = 0.2[m] : \omega = 349.171[1/s]. \quad (22)$$

C. Eigenmode

The eigenmodes corresponding to the eigenfrequencies are

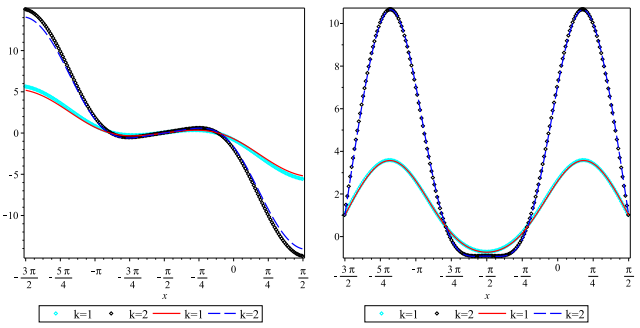

FIG. 30: Eigenmode of displacement u, w, left is for U and right is for W. The point-line represents the mode for case in 4.2 and solid-line represents the case in 4.1.

The results indicate that the eigenfrequency in case of 4.1 and 4.2 has a big difference, while the eigenmode has little difference for literal motion w and small off alignment for mid-surface motion u. The big frequency difference implies that the acceleration in u direction can not be omitted for vibration of torus.

It is worth to mention that such analysis has not been reported in the literature, other shell's vibration can be seen in a famous book by A W Leissa 1993. [40]

V. VERIFICATION OF OUR RESULTS BY FINITE ELEMENT ANALYSIS

A. vs. Finite element analysis

To verify our result, we carried out a finite element analysis for the case study in Section 5.1. The comparisons are shown in Fig. 31. The finite element results

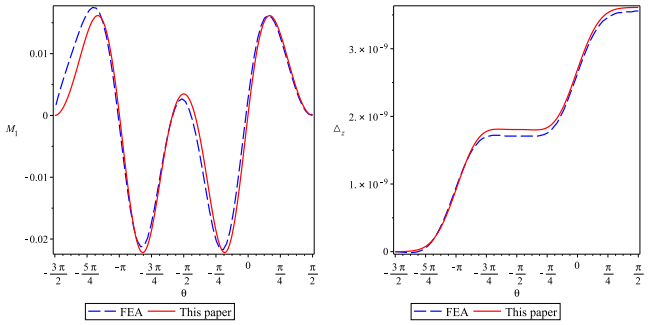

FIG. 31: Results for torus radius with $a = 0.36[m]$ in Section 5.1, as shown in Fig. 5. Left: Bending moment M_1; Right: Vertical displacement Δ_z, this paper gives $\Delta_z(\pi/2) = 3.61080495828841 \times 10^{-9}[m]$, FEM gives $\Delta_z(\pi/2) = 3.557581142 \times 10^{-9}[m]$.

were simulated by ABAQUS with shell element S4R. We applied the boundary condition $\triangle_z(-3\pi/2) = 0$ to cancel the rigid body motion, which might be the reason for minor differences in the range $\theta \in [-3\pi/2, -5\pi/4]$. From physics point of view, our result is symmetric respect to the axes of $\theta = -\pi/2$ while the FEA has slightly symmetry breaking. Therefore, our results are more trustable since the finite element analysis supports our numerical prediction nicely.

B. Comparison with Hans Reisnner's formulation of torus

In the theory of shells of revolution under axisymmetric load, according to Timoshenko and Woinowsky-Krieger 1959 [14], the decisive step was the introduction of N_1 and χ as unknowns by H. Reissner 1912 [25]. The idea has been much extended by E. Meissner 1925 [26]. The formulation of Reissner-Meissner of shells of revaluation

Preprints (www.preprints.org) | NOT PEER-REVIEWED | Posted: 25 January 2022 doi:10.20944/preprints202103.0326.v2

with constant thickness can be found in the masterpieces of Flügge 1973 [15]. All notations in this subsection can be found in Flügge's book [15].

The balance equations are:

$$\frac{R_2}{R_1}\frac{d^2\chi}{d\theta^2}+[\frac{R_2}{R_1}\cot\theta+\frac{d}{d\theta}(\frac{R_2}{R_1})]\frac{d\chi}{d\theta} -(\frac{R_1}{R_2}\cot^2\theta+\mu)\chi=\frac{1}{B}R_1R_2N_1, \tag{23}$$

$$\frac{R_2}{R_1}\frac{d^2}{d\theta^2}(R_2N_1)+[\frac{R_2}{R_1}\cot\theta+\frac{d}{d\theta}(\frac{R_2}{R_1})]\frac{d}{d\theta}(R_2N_1) -(\frac{R_1}{R_2}\cot^2\theta-\mu)(R_2N_1) =-B(1-\mu^2)R_1\chi+Pg(\theta), \tag{24}$$

where χ is the angle by which an element $rd\theta$ of the meridian rotates during deformation; $r=R_2\sin\theta$, the load term P is constant to be determined by the value of $T_1(\pi/2)=-\frac{P}{2\pi R_2}$ and $g(\theta)=\frac{1}{2\pi\sin^2\theta}[\frac{R_1^2-R_2^2}{R_1R_2}\cot\theta+\frac{d}{d\theta}(\frac{R_2}{R_1})]$. The resultant membranae forces can be represented by shear force N_1: $T_1=-N_1\cot\theta-\frac{P}{2\pi R_2}\frac{1}{\sin^2\theta}$, $T_2=-\frac{1}{R_1}\frac{d}{d\theta}(R_2N_1)+\frac{P}{2\pi R_1}\frac{1}{\sin^2\theta}$.

Substituting the principal radii, ie., R_1, R_2 into Eq.23 will give governing equation for torus as follows:

$$\frac{R+a\sin\theta}{a\sin\theta}\frac{d^2\chi}{d\theta^2}+[\frac{R+a\sin\theta}{a\sin\theta}\cot\theta+\frac{d}{d\theta}(\frac{R+a\sin\theta}{a\sin\theta})]\frac{d\chi}{d\theta} -(\frac{a\sin\theta}{R+a\sin\theta}\cot^2\theta+\mu)\chi=\frac{1}{B}a(a+\frac{R}{\sin\theta})N_1, \tag{25}$$

$$\frac{R+a\sin\theta}{a\sin\theta}\frac{d^2}{d\theta^2}[(a+\frac{R}{\sin\theta})N_1] +[\frac{R+a\sin\theta}{a\sin\theta}\cot\theta+\frac{d}{d\theta}(\frac{R+a\sin\theta}{a\sin\theta})]\frac{d}{d\theta}[(a+\frac{R}{\sin\theta})N_1] -(\frac{a\sin\theta}{R+a\sin\theta}\cot^2\theta-\mu)(a+\frac{R}{\sin\theta})N_1 =-B(1-\mu^2)a\chi+Pg(\theta). \tag{26}$$

Once we obtain the shear force N_1 and rotation χ, one can compute all other quantities, such as $T1$, T_2, M_1, M_2, as well as u, w. The problem of elastic torus becomes to find the shear force N_1 and rotation χ from Eq.25 and 26. Obviously, Eq.25 and 26 are complicated and hard to be solved analytically.

TABLE V: Data of torus

Quantities	R	a	h	E	ν	Q_0
Units	m	m	m	N/m^2	1	N
Data	30	10	$a/15$	2.0×10^{11}	0.3	1

To verify our numerical results, for torus with data in Table V, we write a Maple code to compute the Eq.25 and 26 numerically. Detailed Reissner's formulation, Maple coding and numerical simulations will be presented in another paper.

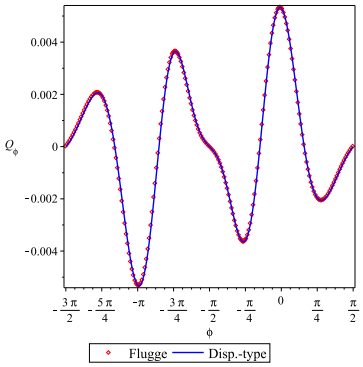

FIG. 32: Displacement form formulation and Hans Reissner's one. Problem as shown in Fig. 5.

The numerical simulation here show that the results Hans Reissner agrees with our displacement formulation, which provides a good supportive evidence about the correctness of our simulation.

VI. CONCLUSIONS

We have reformulated elastic torus in terms of displacement and successfully solved three typical problems and free vibration of torus. To verify our formulation, we wrote a computational code in Maple and carried out some numerical simulations. The validation of our numerical results was confirmed and supported by both finite element analysis and Reissner's formulation. Our investigations show that both deformation and stress response of an elastic torus are sensitive to the radius ratio, and suggest that the analysis of a torus should be done by using the bending theory of a shell, and also reveal that the inner torus is stronger than outer torus due to the property of their Gaussian curvature. Concerning the free vibration of torus, our analysis indicates that both initial in u and w direction must be included otherwise will cause big errors if initial in u direction were omitted. One of the most amazing discovery is that the crowns of a torus are the point of turning point of the Gaussian curvature at $\phi=0$, π, where the mechanics response of inner and outer torus is almost separated.

Acknowledgement:

The author is honored to have benefits from my supervisor Prof. Dr.Ing Wei Zhang (Wei Chang), who was the first Chinese scholar studied the deformation of torus, it is my privilege to dedicate this paper to the memories of Prof. Zhang for his great contribution to the analysis of elastic torus. The author appreciates my students: Mr. Guang-Kai Song, for providing finite

element analysis data in Fig. 31; Mr. Xiong Li, for preparation of Fig.2 (a), Jie Wei for drawing of Fig.2 (b) and Fig.3 (a,b). I also wish to express my gratitude to anonymous reviewers for their high-level academic comments that helps me to enhance the quality of this paper.

Data availability The data that support the findings of this study are available from the corresponding author upon reasonable request.

Conflict of interest The author declares that he has no known competing financial interests or personal relationships that could have appeared to influence the work reported in this paper.

[1] W. Chang (W. Zhang), Derspannungszustand in kreisringschale und ähnlichenSchalen mit Scheitelkreisringen unter drehsymmetrischer Belastung. Arbeitzur Erlangung des Grades eines Doctor-Ingenieurs der Technichen Hochschule, Berlin, 1944.(Sci. Rep Nat. Tsinghua Univ., Ser A. 259-349 (1949))

[2] W.Z. Qian and S.C. Liang, Complex form equation and asymptotic solution. J. of Tsinghua University, 19(1979)(1) 27-47,

[3] Z.H. Xia and W. Zhang, The general solution for thin-walled curved tubes with arbitrary loadings and various boundary conditions. Int. J. Pressures and Piping 26(1986) 129-144.

[4] W. Zhang, W.M. Ren and B. Sun, Toroidal Shells - history, current situation and future. Fifth Conf. of Space Structures, Lanzhou, China 1990.

[5] R.J. Zhang and W. Zhang, Turning point solution for thin toroidal shell vibrations. Int. J. Solids Structures 27(1991)(10) 1311-1326.

[6] R.J. Zhang and W. Zhang, Toroidal shells under nonsymmetric loading. Int. J. Solids Structures, 31(1994) 2735-2750.

[7] B. Audoly and Y. Pomeau, Elasticity and Geometry. University of Cambridge, Cambridge, 2010

[8] B.H. Sun, Closed-form solution of axisymmetric slender elastic toroidal shells. J. of Engineering Mechanics, 136 (2010) 1281-1288.

[9] B.H. Sun, Toroidal Shells. (Nova Novinka, New York, 2012)

[10] R.A. Clark, R.A. and E. Reissner, Bending of curved tubes, Advances in Applied ;Hechanics. vol.II, Academic Press (1950)

[11] R.A. Clark, On the theory of thin elastic toroidal shells. J. Mech. Phys. Solids, 29(1950) 146-178.

[12] N.C. Dahl, Toroidal-shell expansion joints. J. of Applied Mechanics, ASME,20(1953) 497-503.

[13] V.V. Novozhilov, The Theory of Thin Shell. (Noordhoff, Groningen, 1959).

[14] S. Timoshenko and S. Woinowsky-Krieger, Theory of Plates and Shells. McGraw-Hill, New York (1959).

[15] Flügge, W., Stresses in Shells. Springer-Verlag Berlin (1973).

[16] Gol'denveizer, A.L., Theory of Elastic thin Shells. Pergamon Press, New York (1961).

[17] B.H. Sun, Centenary studies of toroidal shells and in memory of Prof. Zhang Wei. Mechanics in Engineering, 37(2013). (In Chinese)

[18] Föppl, L., Vorlesungen Über Technische Mechanik. volume 5.B.G. Teubner, Leipzig, Germany (1907).

[19] G. Weihs. Über Spannungs- und Formänderungszustände in dünnen. Hohlreifen. Halle a. S. 1911.

[20] H. Wissler, Festigkeiberechung von Ringsflachen. Promotionarbeit, Zurich (1916). https://doi.org/10.3929/ethz-a-000099037

[21] V.V. Kuznetsov and S.V. Levyakov, Nonlinear pure bending of toroidal shells of arbitrary cross-section. Int. J. of Solids and Structures, 38(2001) 7343-7354.

[22] A. Zingoni, N. Enoma and N. Govender, Equatorial bending of an elliptic toroidal shell. Thin-Walled Structures, 96(2015) 286-294.

[23] W. Jiammeepreecha and S. Chucheepsakul, Nonlinear static analysis of an underwater elastic semi-toroidal shell. Thin-Walled Structures, 116(2017) 12-18.

[24] N. Enoma and A. Zingoni, Analytical formulation and numerical modelling for multi-shell toroidal pressure vessels. Computers and Structures, 232(2020), Article 105811.

[25] H. Reissner, Spannungen in Kugelschalen (Kuppeln). Festschrift Heinrich Müller-Breslau (A. Kröner, Leipzig, 1912), 181-193

[26] E. Meissner,Über und Elastizitat Festigkeit dunner Schalen. Viertelschr. D. nature.Ges., Bd.60, Zurich (1915).

[27] F. Tölke, Ingenieur Archiv., 9 (1938), 282

[28] E. Reissner, On bending of curved thin-walled tubes. Proc. National Academy of Sci., (1949) 204-208.

[29] L.N. Tao, On toroidal shells. J. of Math. and Physics, 38,(1959) 130-134.

[30] C.R. Steele, Toroidal pressure vessels. J. Spacecr. Rockets., 2(1965) 937-943,

[31] B.H. Sun, Exact solution of Qian's equation of slender toroidal shells. Mechanics in Engineering, 38(2018)(5) 567-569.(in Chinese)

[32] B.H. Sun, Small symmetrical deformation of thin torus with circular cross-cection. Thin-Walled Structures 163 (2021) 107680.

[33] B.H. Sun, Geometry-induced rigidity in elastic torus from circular to oblique elliptic cross-section, Int.J. of Nonlinear Mechanics 135 (2021) 103754.

[34] B. H. Sun, Gol'denveizer's problem of elastic torus. Thin-

 doi:10.20944/preprints202103.0326.v2

Walled Structures, 171 (2022) 108718.
[35] A. Ronveaux, Heun's Differential Equations. Oxford University Press (1995).
[36] https://en.wikipedia.org/wiki/Heun_function
[37] J.E. Marsden, L. Sirovich and S.S. Antman eds. Hypergeometric Functions and Their Applications. Texts in Applied Mathematics. 56. New York: Springer-Verlag (1991).
[38] J.N. Reddy, Theory and Analysis of Elastic Plates and Shells. CRC Press, 2007.
[39] Marple https://www.maplesoft.com/
[40] A.W. Leissa, Vibration of Shells.Acoustical Scociety of America, 1993.

Maple code

```
restart;
with(plots);with(student):
for k to 2 do
a := 0.1*k;
R := 1;
alpha := a/R;
h := a/15;
mu := 0.3;
E := 0.2*10E12;
rho := 8050*9.81;
K := E*h/(-mu*mu + 1);
B := E*h*h*h/(12*(-mu*mu + 1));
q1 := rho*h*lambda*u(x);
qn := rho*h*lambda*w(x);
sun1 := T1(x) - E*h*(mu*(u(x)*cos(x) + w(x)*sin(x))/(R*(1 + a*sin(x)/R)) + (diff(u(x), x) + w(x))/a)/(-mu*mu + 1) = 0;
sun3 := M1(x) - E*h*h*h*(mu*cos(x)*(-diff(w(x), x)/a + u(x)/a)/(R + a*sin(x)) + (-diff(w(x), x, x)/a + diff(u(x), x)/a)/a)/(-12*mu*mu + 12) = 0;
sun5 := N1(x) - (a*cos(x)*M1(x) + (R + a*sin(x))*diff(M1(x), x) - a*cos(x)*E*h*h*h*(mu*(-diff(w(x), x, x)/a + diff(u(x), x)/a)/a + cos(x)*(-diff(w(x), x)/a + u(x)/a)/(R + a*sin(x)))/(-12*mu*mu + 12))/(a*(R + a*sin(x))) = 0;
sun6 := a*cos(x)*T1(x) + (R + a*sin(x))*diff(T1(x), x) - a*cos(x)*E*h*(mu*(diff(u(x), x) + w(x))/a + (u(x)*cos(x) + w(x)*sin(x))/(R*(1 + a*sin(x)/R)))/(-mu*mu + 1) + (N1(x)/a + q1)*a*(R + a*sin(x)) = 0;
sun7 := a*cos(x)*N1(x) + (R + a*sin(x))*diff(N1(x), x) - (T1(x)/a + E*h*(mu*(diff(u(x), x) + w(x))/a + (u(x)*cos(x) + w(x)*sin(x))/(R*(1 + a*sin(x)/R)))*sin(x)/((-mu*mu + 1)*(R + a*sin(x))))*a*(R + a*sin(x)) + qn*a*(R + a*sin(x)) = 0;
equs := sun1, sun3, sun5, sun6, sun7;
bc := T1(Pi/2) = 0, T1(-(3*Pi)/2) = 0, M1(Pi/2) = 0, M1(-(3*Pi)/2) = 0, N1(Pi/2) = 0, N1(-(3*Pi)/2) = 0, w(-3*Pi/2) = 0.00001;
sys := bc, equs;
vars := M1(x), N1(x), T1(x), u(x), w(x);
sol := dsolve(sys, vars, numeric, abserr = 0.1*E-5, output = listprocedure);
M[1][k] := rhs(sol[2]);
N[1][k] := rhs(sol[3]);
T[1][k] := rhs(sol[4]);
hori[k] := rhs(sol[5])*cos(x) + rhs(sol[6])*sin(x);
verti[k] := -rhs(sol[5])*sin(x) + rhs(sol[6])*cos(x);
ur[k] := rhs(sol[5]);
wr[k] := rhs(sol[6]);
print(k);
end do;
```